25th ABCM International Congress of Mechanical Engineering
October 20-25, 2019, Uberlândia, MG, Brazil

COB-2019-0168
PARAMETERIZATION OF TIRE MODEL FOR LIGHT WEIGHT VEHICLE REGARDING THE COMBINED SLIP

Davi Alves de Mendonça
Fabio Mazzariol Santiciolli
Ludmila Corrêa de Alkmin e Silva
Jony Javorski Eckert
Franco Giuseppe Dedini
Integrated Systems Laboratory, University of Campinas - UNICAMP, 200 Mendeleyev Street, Campinas, 13083970, SP, Brazil
d169729@dac.unicamp.br, fabio@fem.unicamp.br, ludmila@fem.unicamp.br, javorski@fem.unicamp.br, dedini@fem.unicamp.br

Abstract. *Nowadays, studies regarding vehicle dynamics study are growing. Concepts of vehicles and autonomous robots amaze enthusiasts of the subject and generate trends for the future. In this contexts, the knowledge about the behavior and reaction forces in the tire have great importance. Small tires are applied in energy efficient vehicles, bicycle, robots and machines. This project studies the dynamic behavior and parameterization of small tires. For this, experimental tests were carried out at the Integrated Systems Laboratory (LabSIn) of the Faculty of Mechanical Engineering of UNICAMP, which has a parameterization bench for small tires. The acquisition of road and tire contact loads and the post-process of the experimental data were carried out. The results of the project are consistent with the literature, and it is possible to notice that the Pacejka model works for light weight vehicle tires regarding the combined slip.*

Keywords: *combined slip, parameterization of tires, light weight vehicle, Pacejka model.*

1. INTRODUCTION

The tire is a component of great importance in vehicle dynamics. It is responsible for the contact between the vehicle and the road, and its characteristics have a great influence on the vehicle performance. According to Ahangarnejad (2018), the vehicle behavior and the performance are strongly related to dynamics of tires. To have a good dynamic analysis and design of the chassis control system, it is necessary an accurate tire dynamic model.

Tire modeling have increased with advance of autonomous vehicle and robots. For this, it is necessary to know the dynamic tire behavior to optimize control efforts. The design of robots through computer-aided engineering was considered one of the strategic topics in the research agenda of the Public Private Partnership in Robotics in Europe, known as SPARC, for the period from 2014 to 2020; tire modeling is fundamental for this and can vary with the characteristics of the tire structure and the ground (Dąbek and Trojnacki, 2016).

The modeling of tire-ground systems have been well established focusing on the automotive industry, which over the years have resulted in the development of several models of tires. However, it has been perceived that mobile robots with wheels, especially light robots, differ significantly from automotive vehicles in terms of applications, maneuvers, terrain types, vehicle design and tire parameters. There is proportionately little work so far in the field of tire-road interaction modeling for lightweight wheel robots (Dąbek and Trojnacki, 2016).

In a previous research, Silva *et al.* (2016) and Silva *et al.* (2017) developed a test bench for the characterization of small tires, registered by patent number PI1004332-2A2 in INPI. Their work obtained good results regarding parameterization of lateral force. Santiciolli (2018) improved the test bench by automating the longitudinal slip, implementing an automated vertical load imposition system and updating the Pacejka model used for the version of 2002; there were good results in lateral and longitudinal forces. Both works showed that Pacejka model behaves well for light weight vehicle regarding the pure slip.

In despite of the achievements of Silva *et al.* (2016), Silva *et al.* (2017) and Santiciolli (2018) regarding the parameterization of the Pacejka model applied to small tires at pure slip, studies about the combined slip were vacant. This paper fills this gap by running a small tire sample at the aforementioned test bench at combined slip conditions and parameterizing the respective Pacejka model. This objective is described in details in Section 2. In Section 3 contains a review about the Pacejka model and the conditions of pure and combined slip. The parameterization of the model facing experimental data is executed by means of a genetic algorithm exposed in Section 4. In Section 5 the reader can find the methodology used to prospect the experimental data and derive the Pacejka model parameterization from them using the genetic algorithm. Finally, the results are exposed and discussed in Section 6 and conclusions are drawn in Section 7.

2. OBJECTIVES

The objective of this study is to parameterize the Pacejka model for a small tire specimen at combined slip situation. To achieve this goal, the specific objectives are:

- Prospect experimental data by testing the small tire specimen in the test bench;
- Obtain the parameterization of this tire specimen regarding pure slip, because it is required for the combined slip parameterization;
- From the whole experimental data, the pure slip parameterization and the generic algorithm, derive the final combined slip parameterization.

3. PACEJKA MODEL

Hans Bastiaan Pacejka proposed the main empirical model of tire known as Magic Formula (MF). This model is based on a sin(arctan) function that not only provides an excellent fit for the curves regarding the Lateral Force (F_x), the Longitudinal Force (F_y) and the Self-aligning Moment (M_z), but also has coefficients that have relationships with shape and magnitude factors of the curves. The general formula is represented in Eq. (1), Eq. (2) and Eq. (3) (Pacejka, 2012).

$$y = Dsin[Carctan(Bx - E(Bx - arctan(Bx)))] \tag{1}$$

$$Y(X) = y(x) + S_V \tag{2}$$

$$x = X + S_H \tag{3}$$

Where Y can be alternatively F_y or M_z with X being the slip angle (α). One can also take Y as F_x with X being the longitudinal slip (κ). The coefficients of the Magic Formula are well defined and responsible for the adjustment of the characteristic curve sin(arctan) at the points obtained experimentally. *B* is the stiffness factor, *C* is the shape factor, *D* is the peak value, *E* is the curvature factor, S_H is the horizontal shift and S_V is the vertical shift. All these coefficients are composed of parameters that change according to the tire shape and structure (Pacejka, 2012).

Pacejka divides the movement of the tire into two conditions. The first one is the pure slip, which is the movement of the wheel when the slip angle is zero and there is only longitudinal slip or when the longitudinal slip is zero and there is only slip angle; these are the situations in which Eq. (1), Eq. (2) and Eq. (3) are valid. The second condition is the combined slip, which happens when there is variation of the slip angle along with the longitudinal slip.

The parameters which compose the coefficients of the Magic Formula are classified into four categories. For longitudinal and lateral force it is used *p* and *r* where *p* is used in pure slip and *r* is used in combined slip.

Table 1. Tire parameters.

LONGITUDINAL FORCE														
p_{Cx1}	p_{Dx1}	p_{Dx2}	p_{Dx3}	p_{Ex1}	p_{Ex2}	p_{Ex3}	p_{Ex4}	p_{Kx1}	p_{Kx2}	p_{Kx3}	p_{Hx1}	p_{Hx2}	p_{Vx1}	p_{Vx2}
p_{Px1}	p_{Px2}	p_{Px3}	p_{Px4}	r_{Bx1}	r_{Bx2}	r_{Bx3}	r_{Cx1}	r_{Ex1}	r_{Ex2}	r_{Hx1}				
LATERAL FORCE														
p_{Cy1}	p_{Dy1}	p_{Dy2}	p_{Dy3}	p_{Ey1}	p_{Ey2}	p_{Ey3}	p_{Ey4}	p_{Ey5}	p_{Ky1}	p_{Ky2}	p_{Ky3}	p_{Ky4}	p_{Ky5}	p_{Ky6}
p_{Ky7}	p_{Hy1}	p_{Hy2}	p_{Vy1}	p_{Vy2}	p_{Vy3}	p_{Vy4}	p_{Py1}	p_{Py2}	p_{Py3}	p_{Py4}	p_{Py5}	r_{By1}	r_{By2}	r_{By3}
r_{By4}	r_{Cy1}	r_{Ey1}	r_{Ey2}	r_{Hy1}	r_{Hy2}	r_{Vy1}	r_{Vy2}	r_{Vy3}	r_{Vy4}	r_{Vy5}	r_{Vy6}			

The combined slip represents the interaction between lateral and longitudinal forces. It is possible to identify this interaction when the vehicle realizes a curve in traction or braking. Pacejka proposed the first model of combined slip in 1987 and improved until the current model finished in 2012 (Pacejka, 2012).

For this condition, Pacejka proposes a weighting function G which indicates the influence of α in the longitudinal force and κ in the lateral force. Then the forces of combined slip can be represented using the equations of pure slip (Y_0).

$$G = Dcos[Carctan(Bx)] \tag{4}$$

$$Y = Y_0 G(\alpha, \kappa, F_z) \tag{5}$$

The function *G* has the parameters exclusive of the combined slip. The Eq. (4) shows a general form of the weighting function and it is adapted for longitudinal force and lateral force where x becomes α and κ respectively. It is possible to put together the curves obtained for a given slip angle and vary the longitudinal slip.

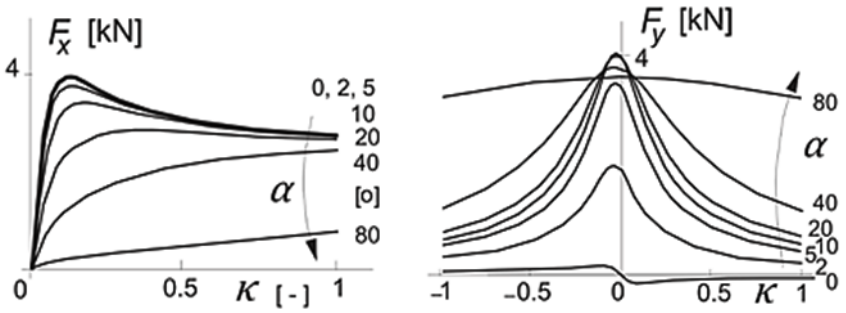

Figure 1. Longitudinal and lateral forces as a function of the variation of κ and α (Pacejka, 2012).

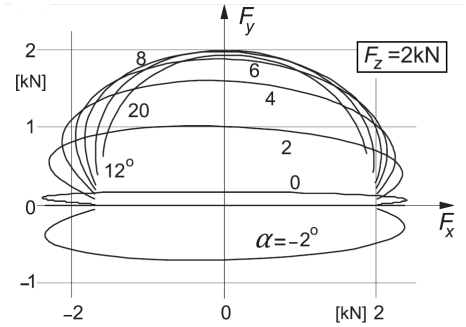

Figure 2. Longitudinal vs lateral forces (Pacejka, 2012).

The Fig. 1 shows that when the slip angle increase, the longitudinal force decreases and the lateral force increases. However when the slip angle is big, the peak lateral force decreases. That happens because in higher angles the tire just slips in the ground and this make the force decrease.

The Fig. 2 represents the lateral force in function of longitudinal force varying the longitudinal slip conditions. When F_x is positive, the vehicle is driving; when it is negative, the vehicle is braking. As the slip angle increases up to a certain value, the curve becomes smoother and the maximum F_x is equal to the maximum F_y.

In the following section, it is explained the use of genetic algorithms to parameterize the Pacejka model from experimental data.

4. GENETIC ALGORITHM

Genetic algorithm is an optimization algorithm based on Darwinian principle of natural selection and genetic operations such as reproduction (crossing over) and mutation. There are four differences between this method and traditional search and optimization methods (Goldberg, 1989):

- Genetic algorithms work with a coding of the parameter set and not with the parameters themselves;
- Search from a population of points, not a single point;
- Use evaluation of goal function, not derivatives or other auxiliary knowledge;
- Use probabilistic transition rules, not deterministic rules.

Cabrera *et al.* (2004) proposes to use a genetic algorithm to find the parameters of the tire, which was named IOA (IMMa Optimization Algorithm). The main benefits of this algorithm are the efficiency with simplicity of implementation and low computational cost. In addition, a previous knowledge about the initial population is not necessary and it can be chosen randomly by the algorithm, a fact that is useful when dealing with MF parameterization.

The objective of this optimization algorithm is to find the parameters that minimize the sum of the square of the difference between the experimental data and Pacejka model, which in combined slip depends of slip angle, longitudinal slip and the vertical force. These goal functions for longitudinal and lateral forces are represented in Eq. (6).

$$min \sum_{i=1}^{n} \sum_{j=1}^{m} \sum_{f=1}^{p} [F_{x,y}^{Pacejka}(X, Y, \alpha_f, \kappa_i, F_{zj}) - F_{x,y}^{measured}(\alpha_f, \kappa_i, F_{zj})]^2 \tag{6}$$

For this, as shown in the Fig. 3, a random generation of starting population with NP individuals is created, where the individuals are the tire parameters. Then, two random individuals and the best individual are selected to form the disturbing vector (V). The disturbing vector is also a function of F, which is a real value that controls the disturbance. This vector is crossed, with a probability defined as CP, with the current population and generates the next population (X_i^N).

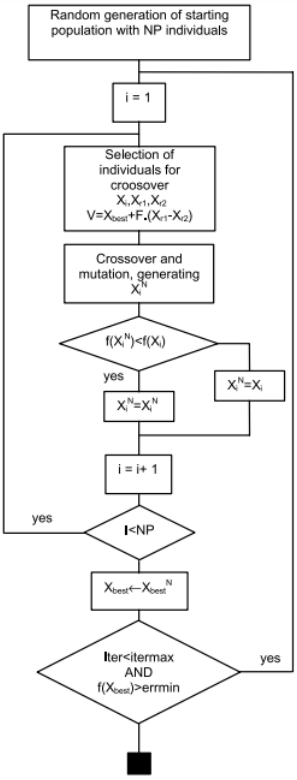

Figure 3. Scheme of genetic algorithm (Cabrera *et al.*, 2004)

The mutation happens simultaneously with the reproduction with a probability defined as MP. In this operation, a aleatory value within a $range$ is added or subtracted from a random individual . If the new population member is better than the current, it is replaced. This algorithmic routine is repeated until the number of iterations reaches the number maximum or the fitness of the best population is lower than the minimum error.

To increase the speed of convergence and achieve a higher percentage of success in the optimization, the four control parameters F, CP, MP and $range$ can be included in the optimization. Thus, the best values of these parameters are found throughout the iterations, without the requirement of the input values (Ortiz *et al.*, 2009).

The next section exposes how the materials are used and how the data acquired is treated according to the aforementioned theory.

5. MATERIALS AND METHODS

In Fig. 4 it is possible to see the arrangement of the current bench basically composed of the table of Honeycomb, three load cells (indicated with 1), two of them transverse and one longitudinal, two electric motors (indicated with 2), where one is a step motor responsible for the translation of the wheel and another is a DC motor responsible for wheel rotation. With the combination of the two motors it is possible to impose the longitudinal sliding. It also contains a vertical pneumatic actuator (indicated with 3) controlled by a proportional pneumatic valve through which it is possible to impose vertical force on the wheel. The bench has some sensors like extensometers and encoders.

The tire specimen selected for this research is a 4PR Imsa tire (shown in Fig. 5). It is normally used for human-traction pallets and it is also suitable for robots.

The experimental tests were conducted to obtain the forces at the tire in different conditions. For this, the 4PR Imsa tire sample was subjected to several tests varying the slip angle, the longitudinal slip and the vertical load. For each test, the longitudinal and lateral forces were acquired. In order to obtain a good parameterization, it was chosen nine different slip angles (-20° to 20°, varying 5°), three different vertical load (60N, 110N and 160N) and eleven different longitudinal slips (from -50% to 100%). Considering this set of experiments, both pure and combined slip conditions are observed.

To carry out the tests, the slip angle was regulated through a ball joint and verified by a scanner, the pressure of the tire was set at 30 psi and the vertical load was imposed by a vertical pneumatic actuator. Then the wheel is moved along the bench where the longitudinal slip is imposed and the forces are measured.

Finally, the equations of Pacejka are fitted to the experimental points, obtaining the parameters of the tire for both pure and combined slip conditions. For this, it was used the genetic algorithm IOA previously explained.

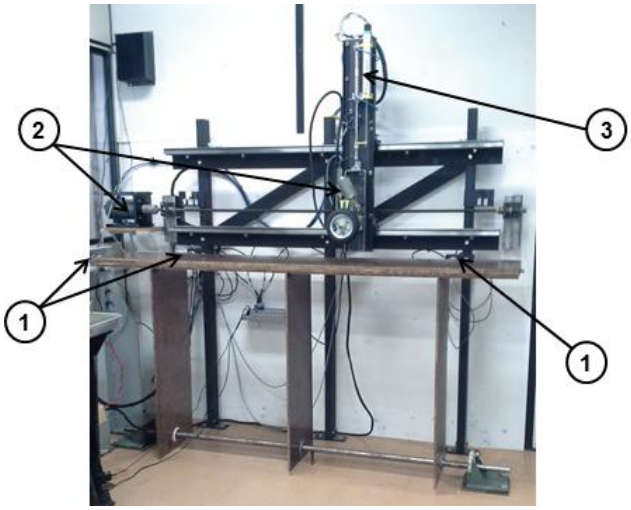

Figure 4. Overview of current bench configuration.

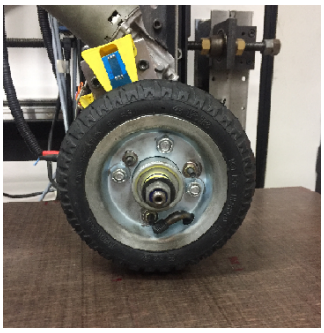

Figure 5. 4PR Imsa Tire, tire size 152,4 x 50,8 mm (diameter x width).

6. RESULTS AND DISCUSSION

The parameters for pure slip were found after 10000 iterations for each force and they are represent in the Tab. 2, where some of them that were not used because they multiply the camber angle, which in this research is always zero. The best equivalent fitness was 155 N^2 and 863 N^2 for longitudinal and lateral forces, respectively. This is a good result in view of the fact that the fitness function is the sum of the square of the error between the experimental data and the IOA curve and there are several points measured.

Table 2. Optimization results of the parameters for pure slip, tire size 152,4 x 50,8 mm (diameter x width).

LONGITUDINAL FORCE									
p_{Cx1}	p_{Dx1}	p_{Dx2}	p_{Dx3}	p_{Ex1}	p_{Ex2}	p_{Ex3}	p_{Ex4}	p_{Kx1}	p_{Kx2}
$0,070$	$-5,941$	$-1,027$	$*$	$0,011$	$-0,063$	$0,023$	$-12,513$	$0,050$	$0,085$
p_{Kx3}	p_{Hx1}	p_{Hx2}	p_{Vx1}	p_{Vx2}	p_{Px1}	p_{Px2}	p_{Px3}	p_{Px4}	
$-0,634$	$0,883$	$-0,806$	$-0,032$	$-0,013$	$1,654$	$0,162$	$-0,090$	$-0,231$	
LATERAL FORCE									
p_{Cy1}	p_{Dy1}	p_{Dy2}	p_{Dy3}	p_{Ey1}	p_{Ey2}	p_{Ey3}	p_{Ey4}	p_{Ey5}	p_{Ky1}
$0,068$	$1,189$	$0,121$	$*$	$-0,019$	$-0,204$	$-3,483$	$*$	$*$	$19,462$
p_{Ky2}	p_{Ky3}	p_{Ky4}	p_{Ky5}	p_{Ky6}	p_{Ky7}	p_{Hy1}	p_{Hy2}	p_{Vy1}	p_{Vy2}
$-68,684$	$*$	$-219,057$	$*$	$-0,098$	$0,859$	$-0,014$	$-0,002$	$0,023$	$-0,095$
p_{Vy3}	p_{Vy4}	p_{Py1}	p_{Py2}	p_{Py3}	p_{Py4}	p_{Py5}			
$*$	$*$	$0,368$	$-1,588$	$13,491$	$-3,076$	$-1,781$			

* not exploited because $\gamma = 0$ [rad]

The curves of longitudinal and lateral forces for different vertical loads, formed by the parameters found with the IOA algorithm and the experimental points were represent in the Fig. 6

Using the Eq. (4) and Eq. (5) the tire parameters for combined slip were found after 10000 iterations for longitudinal

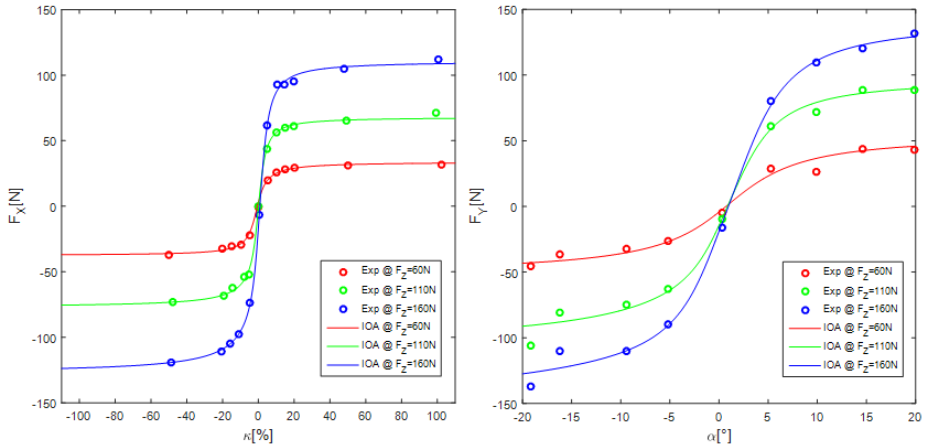

Figure 6. Longitudinal and lateral forces for pure slip

and lateral forces. The values of parameters for combined slip do not have a clear meaning because they are very coupled in the weighting function G. The Tab. 3 shows the parameters for combined slip found in the parameterization.

Table 3. Optimization results of the parameters for combined slip, tire size 152,4 x 50,8 mm (diameter x width).

LONGITUDINAL FORCE							
r_{Bx1}	r_{Bx2}	r_{Bx3}	r_{Cx1}	r_{Ex1}	r_{Ex2}	r_{Hx1}	
$261,6407$	$-3,7956$	$*$	$0,8669$	$-0,1240$	$-1,0637$	$-0,0157$	
LATERAL FORCE							
r_{By1}	r_{By2}	r_{By3}	r_{By4}	r_{Cy1}	r_{Ey1}	r_{Ey2}	r_{Hy1}
$3,1056E4$	$-3,1780E6$	$0,0050$	$*$	$-0,9844$	$0,1370$	$-0,0164$	$1,0579$
r_{Hy2}	r_{Vy1}	r_{Vy2}	r_{Vy3}	r_{Vy4}	r_{Vy5}	r_{Vy6}	
$-0,9666$	$984,5821$	$30,4729$	$*$	$1,6779E7$	$49,8457$	$55,0112$	

$*$ not exploited because $\gamma = 0$ [rad]

After the 10000 iterations, the best equivalent fitness for longitudinal force was 1,7022E4 N^2 and the best for lateral force was 9,9421E3 N^2. These fitness are higher than pure slip because in this case the number of points is higher.

With these parameters it was possible post-processing with the MF and form surfaces for different vertical loads. The surface evidences the influence of longitudinal slip and slip angle. The discreteness of the mesh was made from -110% to 110% (varying 4%) and $-20°$ to $20°$ (varying $5°$), respectively. The experimental points are represented with a cross and each color is one test carried out.

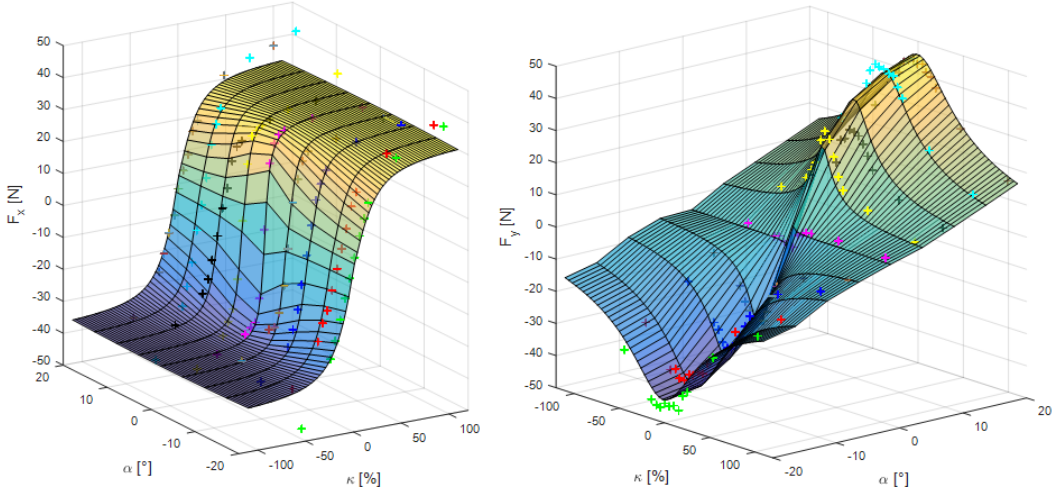

Figure 7. Longitudinal and lateral surfaces for $F_z = 60N$.

Comparing the Fig. 7, Fig. 8 and Fig. 9 it is possible to notice that they have a similar form. This occurs because the only difference between them is the vertical load. When the vertical load is bigger, the modules of longitudinal and

lateral force increase. Furthermore, the surface of longitudinal force shows that when the slip angle is close to $0°$ the longitudinal curve is more pronounced and when the slip angle is away from $0°$ the curve is smoother. This behaviour is easily observed by looking at the lines parallel to the slip angle, where for the same longitudinal slip the longitudinal force gets more intensive close to $0°$.

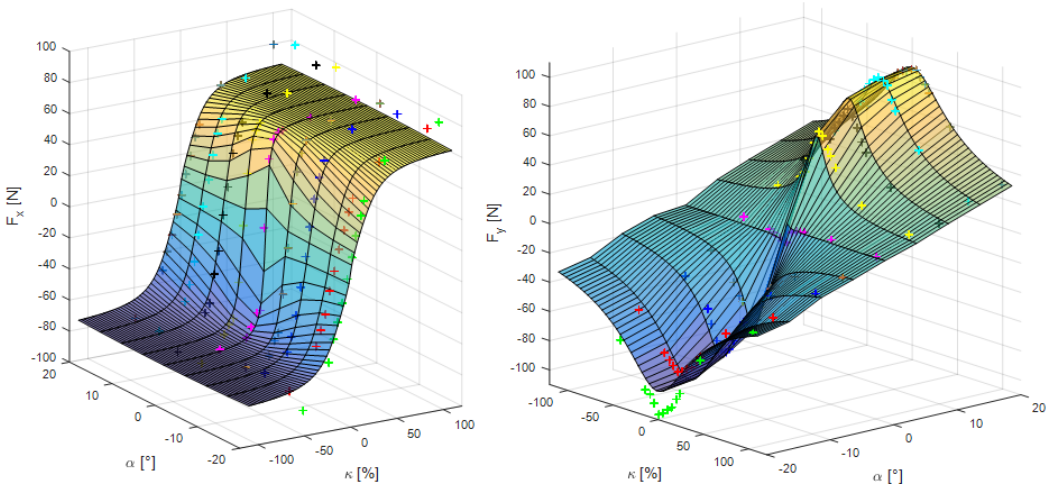

Figure 8. Longitudinal and lateral surfaces for $F_z = 110N$.

For the lateral force, the response was very satisfactory with higher lateral force for the higher slip angles. Other interesting observation is the inversion of the curves when the slip angle comes from positive to negative values (and vice versa). In addition, it is possible to note that the lateral force is almost zero when the slip angle is $0°$ because the geometry favors longitudinal force.

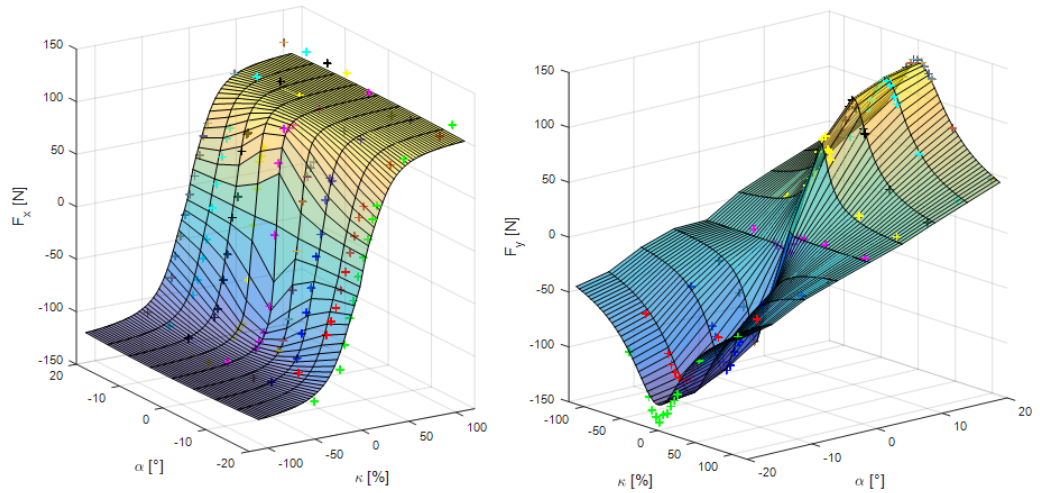

Figure 9. Longitudinal and lateral surfaces for $F_z = 160N$.

For all the three vertical forces the IOA surfaces has a great adjustment with the experimental data. Especially for values of κ between -50% and 50% for longitudinal force. This is not a problem because for almost all applications, the longitudinal slip is in this range. Besides, the amplitude for positive and negative conditions of slip angle and longitudinal slip are coherent, having the same module and neutralizing the outlier points.

Other interesting result to identify the interaction between longitudinal and lateral force is shown in the Fig. 10. It is possible to notice that the curves are similar varying the vertical load and they are very smooth. This explains why the longitudinal force does not present a peak as the longitudinal slip increases (alternatively to what happens in automotive graphics), but it tends to settle to a constant.

Then, when the vehicle starts a curve, the longitudinal slip is approximately zero, and there is only lateral force. As the vehicle accelerates or brakes, the longitudinal slip increases or decreases, respectively, in order to keep the lateral force constant and the slip angle increases. There is a extreme point, when the F_x is maximum for constant F_y, that the tire loses the grip. Then if the vehicle releases the brake or the accelerator the grip returns, the longitudinal slip decreases (along the curve with constant α) and the longitudinal force returns to zero but now with a higher slip angle, which implies in a higher lateral force.

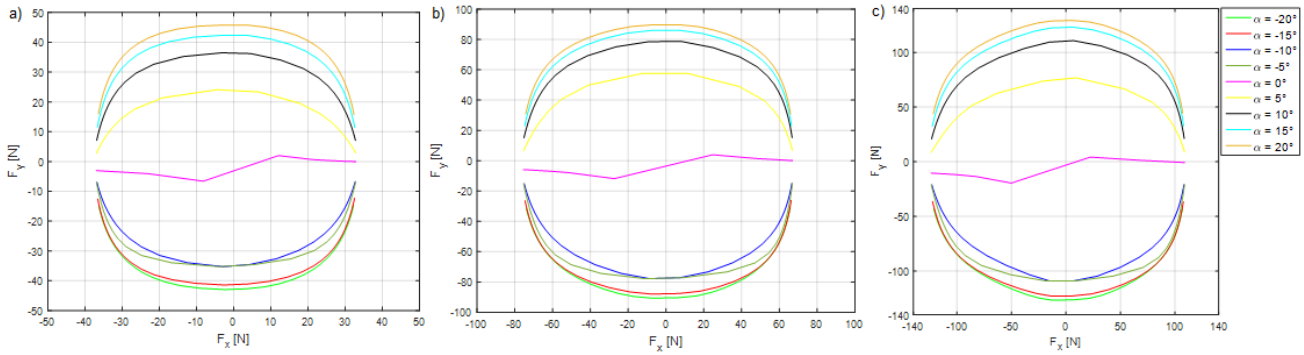

Figure 10. Lateral force vs longitudinal force for a) $F_z = 60N$, b) $F_z = 110N$ and c) $F_z = 160N$.

7. CONCLUSION

In this paper it was performed the parameterization of Pacejka tire model for a light weight vehicle regarding the combined slip. For this, the parameterization for a pure slip in the same conditions of pressure and vertical loads was made and after the complete parameterization for the combined slip was executed.

The results were obtained by fitting the experimental data with the Pacejka model through the genetic algorithm IOA. Then all the parameters for longitudinal and lateral forces, disregarding the camber angle, were obtained. The great adjustment showed that the Pacejka model works correctly for combined slip and pure slip for a light weight vehicle tire.

The main difference noted between the light weight vehicle tire and automotive tire in the parameterization is that for the longitudinal force there is not a peak of the force for medium longitudinal slip. Then the light weight vehicle will lose the grip before the automotive tire because it does not have the peak in longitudinal force. This shows the importance of using a parameterization for small tires instead of using an automotive tire as an approximation.

With the complete parameterization for pure and combined slip it is possible use these parameters for a similar tire by finding the scaling factors, which can be achieved by adjusting the model for the different tire and/or ground set.

8. ACKNOWLEDGEMENTS

The authors thank the National Council for Scientific and Technological Development (CNPq), Brazilian Federal Agency for Support and Evaluation of Graduate Education (CAPES), State of São Paulo Research Foundation (FAPESP) and the University of Campinas (UNICAMP) for infrastructural and financial support.

9. REFERENCES

Ahangarnejad, A.H., 2018. *Integrated control of active vehicle chassis control systems*. Ph.D. thesis, Politecnico Di Milano, Milan, Italy.

Cabrera, J.A., Ortiz, A., Carabias, E. and Simon, A., 2004. "An alternative method to determine the magic tyre model parameters using genetic algorithms". *Vehicle System Dynamics*, Vol. 41, No. 2, pp. 109–127.

Dąbek, P. and Trojnacki, M., 2016. "Requirements for tire models of the lightweight wheeled mobile robots". In *Mechatronics: Ideas, Challenges, Solutions and Applications*. Warsaw, Poland.

Goldberg, D.E., 1989. *Genetic Algorithms in Search, Optimization, and Machine Learning*. Addison-Wesley, Massachusetts, 1st edition.

Ortiz, A., Cabrera, J.A., Guerra, A. and Simon, A., 2009. "The imma optimisation algorithm without control input parameters". *Vehicle System Dynamics*, Vol. 47, No. 2, pp. 243–264.

Pacejka, H.B., 2012. *Tire and Vehicle Dynamics*. Butterworth-Heinemann, Oxford, 3rd edition.

Santiciolli, F.M., 2018. *Parametrização de modelos de pneus aplicados a pneus de pequeno porte*. Ph.D. thesis, Universidade Estadual de Campinas, Campinas, Brazil.

Silva, L.C.A., Corrêa, F.C., Eckert, J.J., Santiciolli, F.M. and Dedini, F.G., 2017. "A lateral dynamics of a wheelchair: identification and analysis of tire parameters". *Computer methods in biomechanics and biomedical engineering*, Vol. 20, No. 3, pp. 332–341.

Silva, L.C.A., Dedini, F.G., Corrêa, F.C., Eckert, J.J. and Becker, M., 2016. "Measurement of wheelchair contact force with a low cost bench test". *Medical Engineering and Physics*, Vol. 38, No. 2, pp. 163–170.

10. RESPONSIBILITY NOTICE

The authors are the only responsible for the printed material included in this paper.